ACS SyntheticBiology

Letter

pubs.acs.org/synthbio

Modular Design of a Synthetic Payload Delivery Device

Jin H. Huh,[†,‡] Josh T. Kittleson,[†,‡] Adam P. Arkin,[†,‡,§,∥] and J. Christopher Anderson*[,†,‡,§,∥]

[†]Department of Bioengineering and [§]QB3: California Institute for Quantitative Biological Research, University of California, Berkeley, California 94720, United States

[‡]Synthetic Biology Engineering Research Center (SynBERC), Berkeley, California 94720, United States

[∥]Physical Biosciences Division, Lawrence Berkeley National Laboratory, Berkeley, California 94720, United States

Supporting Information

ABSTRACT: Predictable engineering of complex biological behaviors using characterized molecular functions remains a key challenge in synthetic biology. To explore the process of engineering biological behaviors, we applied a modular design strategy to the development of *E. coli* that deliver macromolecules to the cytoplasm of cancer cells *in vitro*. First, we specified five abstract, qualitative behaviors that would act in concert to achieve payload delivery. Drawing from disparate sources of previously described genetic components, we then designed, constructed, and tested individual genetic circuits to implement each module. Subsequent coupling of the modules and system optimization, aided by quantitative predictions, generated a system that delivers proteins to 80% of targeted cancer cells. Development of an effective delivery system provides strong evidence that advanced cellular behaviors, not just transcriptional circuits, can be rationally decomposed into a series of functional genetic modules and then constructed to achieve the target activity with the existing synthetic biology toolkit.

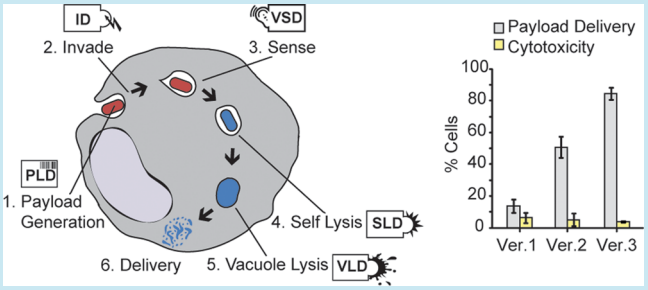

KEYWORDS: *synthetic biology, system level engineering, modular design, payload delivery, tumor-killing bacterium*

Synthetic biologists engineer genetic circuits for applications ranging from biosynthesis to biotherapeutics.[1] Although the application of engineering strategies such as standardization, abstraction, and modularity has long been highlighted as the path to designing complex biological systems,[2] early work generally relied on an *ad hoc* strategy, limiting applications to relatively simple systems.[3] More recently, several groups have explicitly applied modular design to the development of biosynthetic pathways,[4] biological computation,[5] and increasingly sophisticated logic functions.[6] However, the challenge of predictably meeting a performance specification using modular design from defined genetic subsystems remains to be met. To elucidate the barriers to such design, we created a modular design specification to engineer *E. coli* that deliver macromolecules to the cytoplasm of cancer cells *in vitro*. This problem is of sufficient complexity that it would be inefficient to use *post hoc* design. Failure or poor performance resulting from construction and testing of the entire system at once would be difficult to troubleshoot. Further, even if the problem were known, the lack of a modular, synthetic infrastructure would hamper replacement of the faulty component with a more effective one. Instead, we divide the system into functional modules, assuming that the modules can be independently fabricated and tested and that the modules will behave predictably when connected together.

Advanced therapeutic strategies, such as gene therapy and highly targeted cancer cell elimination, rely on intracellular delivery of biological macromolecules. Due to the instability of important biomolecules in extracellular milieu, several strategies for protecting biomolecules have been proposed.[7] Bacterial delivery systems have been used for direct modification of mammalian cells,[8] for delivery of biotherapeutics for cancer and probiotic applications, and as a vector for systems where traditional genetic delivery methods are insufficient.[9] They can process information *in situ*, synthesize relevant biomolecules, and access difficult to reach cell populations.[10] Several examples of engineered bacteria have been described based on attenuated *Listeria monocytogenes* and other pathogens.[11−14] However, use of any attenuated pathogen runs the risk that it will recover or retain uncontrolled aspects of its virulence, rendering this approach infeasible as a general solution. To address this problem, nonpathogenic *E. coli* have been explored as a potential delivery vehicle[15] for therapeutic applications including gene therapy and cancer treatment.[16] Functional DNA has been delivered to a variety of mammalian cell lines[9,17,18] by employing mutations in the native diaminopimelic acid (DAP) synthesis pathway that cause dividing bacteria to lyse in phagosomes. However, bacteria can persist unlysed inside of lysosomes for over 24 h,[17] presumably due to growth stasis in nutrient-limited phagocytic vacuoles. Combined with the operational complexity of continuously

Received: October 9, 2012
Published: February 27, 2013

 © 2013 American Chemical Society

providing DAP, this limits the applicability and efficiency of current *E. coli*-based techniques and additional refinement of this approach is needed to achieve therapeutic value *in vivo*.[9] Here, we circumvent DAP mediated lysis by applying modular design principles to engineer *E. coli* that actively lyse themselves and the phagocytic vacuole in response to the vacuole microenvironment.

We first specified the desired high-level system behavior. Delivery starts with invasion of the bacterium into the mammalian cell, resulting in bacterial uptake into a vacuole (Figure 1a). After recognizing the vacuole microenvironment, the bacterium lyses itself and the vacuole, delivering bacterial macromolecules into the cytosol. Given the high complexity of constructing the entire system *de novo* as a single genetic program, we instead used the temporal separation of events to decompose the system into five functional modules: a payload device (PLD) that generates macromolecules for delivery, an invasion device (ID) that initiates bacterial uptake into the mammalian cell, a vacuole sensing device (VSD) that responds to the vacuolar microenvironment, a self-lysis device (SLD) that causes bacterial lysis, and a vacuole lysis device (VLD) that ruptures the vacuole. Together, the ID, VSD, SLD, and VLD modules comprise a complete genetic program (the Payload Delivery Device, PDD) for delivery of macromolecules generated by the PLD.

Guided by the module descriptions, we selected genetic components with known biochemical activities to implement each of the five modules. For modules with unclear engineering requirements or limited prior characterization in diverse contexts, we examined multiple device variants. The PLD expresses two fluorescent proteins that enable visual tracking of delivery to the mammalian cell (PLD, Figure 1b). Upon release into the mammalian cytoplasm, RFP distributes throughout the cytoplasm, while NLS[19]-GFP concentrates in the nucleus. The ID consists of constitutively expressed invasin (*inv*) from *Yersinia pseudotuberculosis*[20] (ID, Figure 1b). Invasin binds to β1-integrins, surface proteins overexpressed by a variety of human cancers,[21] and induces bacterial uptake by phagocytosis.[22] In Figure 2a, several bacteria bearing the ID have been phagocytosed by a human carcinoma cell (HeLa). This result is consistent with previous work[20] and confirms that the ID independently confers an invasive phenotype. The VSD must differentiate between encasement within a vacuole and other growth environments. Based on the behavior of invasive pathogens,[23] we reasoned that PhoPQ responsive promoters, likely responding to low Mg^{2+} in the vacuole,[24] would serve as an appropriate trigger. We measured the Mg^{2+}-repressed (off-state) and Mg^{2+}-starved activity (on-state) of a known PhoPQ responsive promoter, P_{phoP} (Figure 3a), confirming its response to Mg^{2+} starvation.

We constructed two SLDs, each employing the holin, antiholin, and lysozyme from either the λ lytic system[25] or the T4 lytic system.[26] In these systems, free holin accumulates, oligomerizes, and forms pores in the inner membrane. Lysozyme then gains access to periplasm through those pores and degrades the peptidoglycan layer, resulting in *E. coli* lysis. Antiholin binds to holin and limits accumulation of lysis-initiating holin oligomers. Because we observed that even tightly regulated (P_{BAD}-controlled) expression of holin and lysozyme alone caused growth instability (data now shown), we pursued an architecture employing antholin to prevent unwanted lysis. In our system, each device consists of a promoterless operon containing holin and lysozyme followed

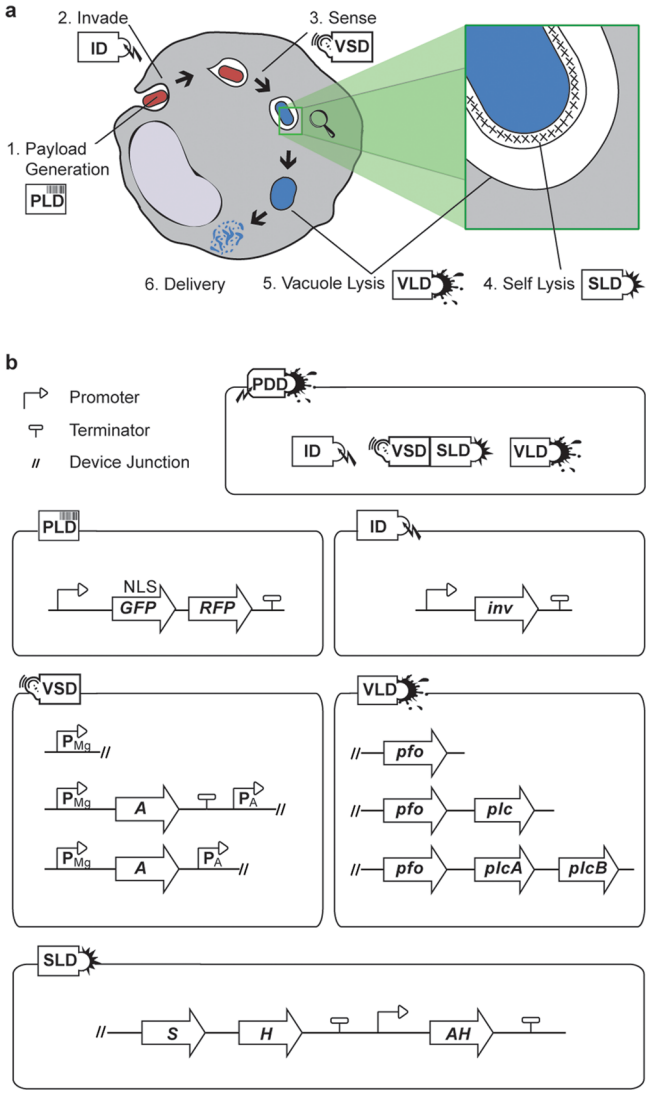

Figure 1. Payload delivery scheme and device composition. (a) Payload proteins are expressed throughout the delivery process (1). An invasion module causes bacterial uptake into a vacuole (2), where the bacterium responds to the vacuolar environment (3). This triggers self-lysis (4) and subsequently vacuole lysis (5), leading to delivery of the payload to the cytoplasm (6). (b) Composition of devices. PDD: payload delivery device. ID: invasion device. VSD: vacuole sensing device. SLD: self-lysis device. VLD: vacuole lysis device. PLD: payload generation device. *NLS*: nuclear localization signal. *GFP*: green fluorescent protein. *RFP*: red fluorescent protein. *inv*: invasin. P_{Mg}: Magnesium responsive promoter. *A*: activator (see Supporting Information). P_A: Activator responsive promoter. *s*: lysozyme. *H*: holin. *AH*: antiholin. *pfo*: perfringolysin O. *plc*: phospholipase C. *plcA*: phosphoinositide (PI)-specific phospholipase C. *plcB*: phosphatidylcholine (PC)-specific phospholipase C.

by a second, constitutively transcribed operon containing antiholin (SLD, Figure 1b). This produces enough antiholin to sequester low levels of holin resulting from leaky basal expression, reducing premature cell death and achieving threshold-gated lysis as described for systems with a similar architecture.[27] To facilitate device integration, conditions identical to those of the VSD assay (both in the presence and absence of Mg^{2+}) were used to measure the effectiveness of the SLDs. The λ device outperformed the T4 device, causing 80% lysis at the highest transcription level tested in the absence

dx.doi.org/10.1021/sb300107h | *ACS Synth. Biol.* 2013, 2, 418−424

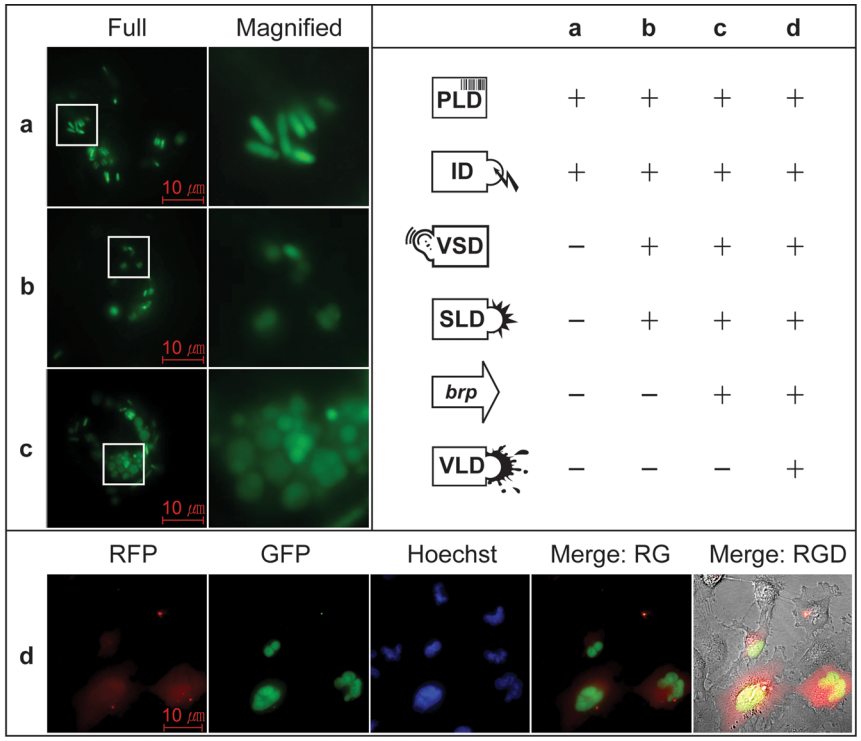

Figure 2. Device and system function *in vivo*. *E. coli* bearing the payload device and one or more other devices were incubated with HeLa (A, B, C) or U373 MG (D) cells and then observed by microscopy. (+): device is installed. (−): device is not installed. (a) The ID only. (b) The ID and the VSD(P_{phoP}) driving the SLD(λ) without BRP. (c) The ID and the VSD(P_{phoP}) driving the SLD(λ) with BRP. (d) The ID, the VSD(P_{mgrBl}) driving a SLD(λ) with BRP, and the VLD(degradation tagged *pfo/plc*) driven by a constitutive promoter, P_{con}.

of Mg^{2+} (Figure 3b). It functioned poorly in the presence of Mg^{2+}, achieving only 20% lysis at the highest transcription level tested. This is consistent with previous observations that lambda phage lacking *Rz* genes fail to lyse host *E. coli* effectively in the presence of divalent cations.[28]

We fabricated VLDs using the cytolysin genes phospholipase C (*plc*) and cholesterol-dependent perfringolysin O (*pfo*) from *Clostridium perfringens*[29] and two phospholipase C genes from *Listeria monocytogenes*, *plcA* and *plcB*[30] (VLD, Figure 1b). In this system, PFO oligomers create pores in the vacuole membrane, allowing PLCs to access the outer leaf of the lipid bilayer, where they initiate degradation of the vacuole membrane. While the activity of PFO is limited to cellular membranes containing cholesterol, leaving *E. coli* cells intact, accumulation of sufficiently high levels of PFO in the mammalian cytoplasm causes cellular lysis.[31] Thus we then added N-terminal degrons,[32] which we expected to prevent unwanted cytosolic activity by targeting the proteins for rapid degradation by the ubiquitin-proteasome pathway. Absent a meaningful *in vitro* experiment to independently test VLD variants, they were only tested once combined with other devices.

Having implemented individual modules, we proceeded to join them into larger systems, starting with the VSD and SLD. Composition of P_{phoP} with the λ SLD generated a device stable in cells in the presence of Mg^{2+} (Figure 4a), but that caused cell lysis in the absence of Mg^{2+} (data not shown). Unexpectedly, cells with the ID, VSD, and SLD failed to completely lyse inside of vacuoles (Figure 2b), instead rounding up but remaining intact. The round cell morphology, perhaps a consequence of a stabilizing factor such as Ca^{2+},[33] is consistent with the outer membrane remaining intact[28] inside the vacuole. We therefore revisited the design of the SLD to include a protein capable of independently lysing the outer membrane. Bacteriocin release protein (BRP) from *E. coli* permeabilizes the outer membrane by activating phospholipase A.[34] After verifying independent BRP function (Supplementary Figure 2), we incorporated BRP into the first, promoterless operon of the original SLD and confirmed maintenance of lysis activity *in vitro* (Figure 3b) and subsequently observed successful delivery of payload to the vacuole *in vivo* (Figure 2c).

We constructed complete payload delivery systems by adding VSD-driven variants of the VLD into cells possessing the ID and VSD-driven SLD and assayed them for delivery efficiency and cytotoxicity (Figure 4b). PFO and PLC with N-terminal degrons had the highest delivery efficiency, delivering the payload to 15% of invaded target cells. However, all device variants had similarly low levels of cytotoxicity, irrespective of the presence of an N-terminal degron, suggesting that the amount of vacuole lysing proteins delivered to the cytosol was below toxic levels. Further, the majority of invaded mammalian cells internalized 1−3 bacteria but contained unlysed vacuoles filled with GFP (data not shown), suggesting insufficient VLD activity. On the basis of these observations, we sought to further improve payload delivery efficiency by decoupling expression of the VLD proteins from the VSD. A strong constitutive promoter driving the VLD increased payload delivery efficiency from 15% to 50% without any increase in cytotoxicity (Figure 4c).

As a final optimization step, we revisited the VSD module, evaluating four derivatives of the P_{phoP} promoter bearing transcriptional amplifiers (composition shown in Figure 1b) and four additional known PhoPQ responsive promoters (P_{mgtCB}, P_{mgtA}, P_{mgtCBI}, and P_{mgrBI}). We expected that successful

dx.doi.org/10.1021/sb300107h | *ACS Synth. Biol.* 2013, 2, 418−424

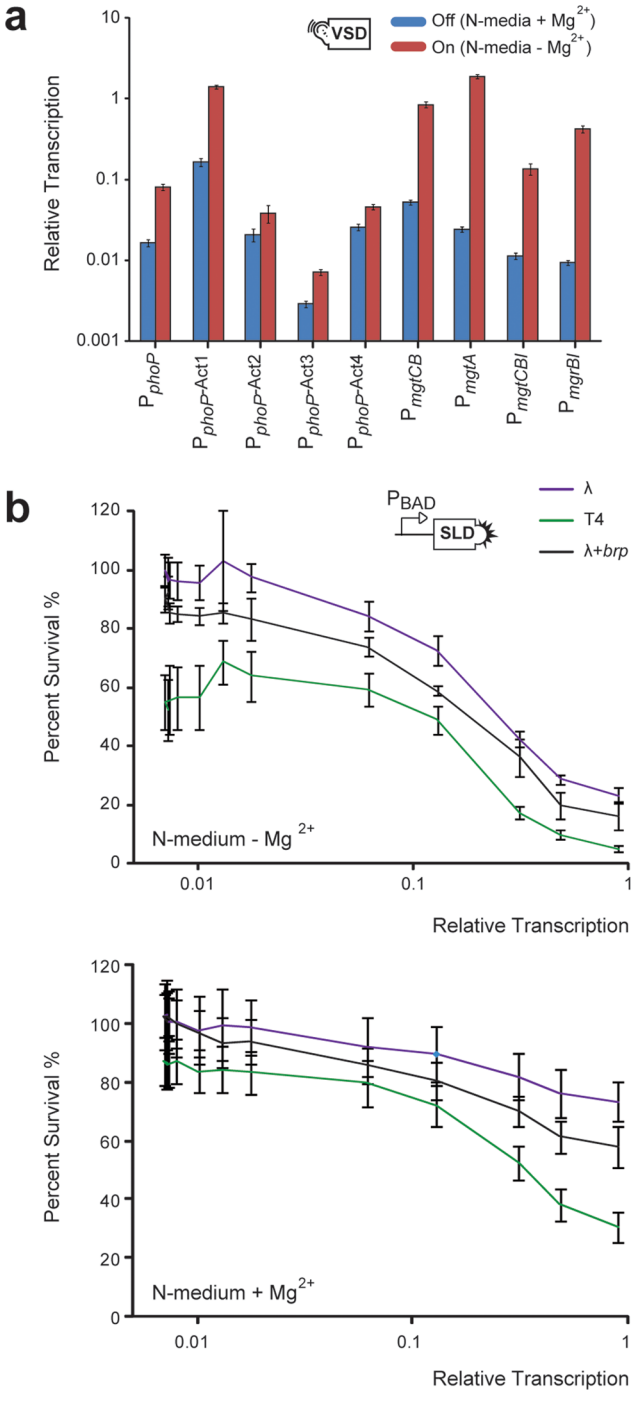

Figure 3. Characterization of individual devices. (a) The induced (On) and uninduced (Off) activity of VSD variants. (b) The lysis efficiency of SLD variants in the presence and absence of Mg^{2+}. Error bars in both panels are the standard deviation of 4 biological replicates.

VSD-SLD combinations could be predicted by measuring the transcription output of the VSD variants (Figure 3a) and calculating the theoretical performance of each of the VSD-SLD combinations (Figure 4a). We performed a preliminary validation of these predictions by measuring the growth rate of cells bearing each device combination (Figure 4a). The two VSDs predicted to cause the highest basal self-lysis activity, P_{mgtCB} and P_{phoP}-act1, in fact showed clear growth defects. P_{phoP}-act2, P_{phoP}-act3, P_{phoP}-act4, P_{mgrBI}, and P_{phoP} driving the SLD grew comparably to the control, consistent with their predicted

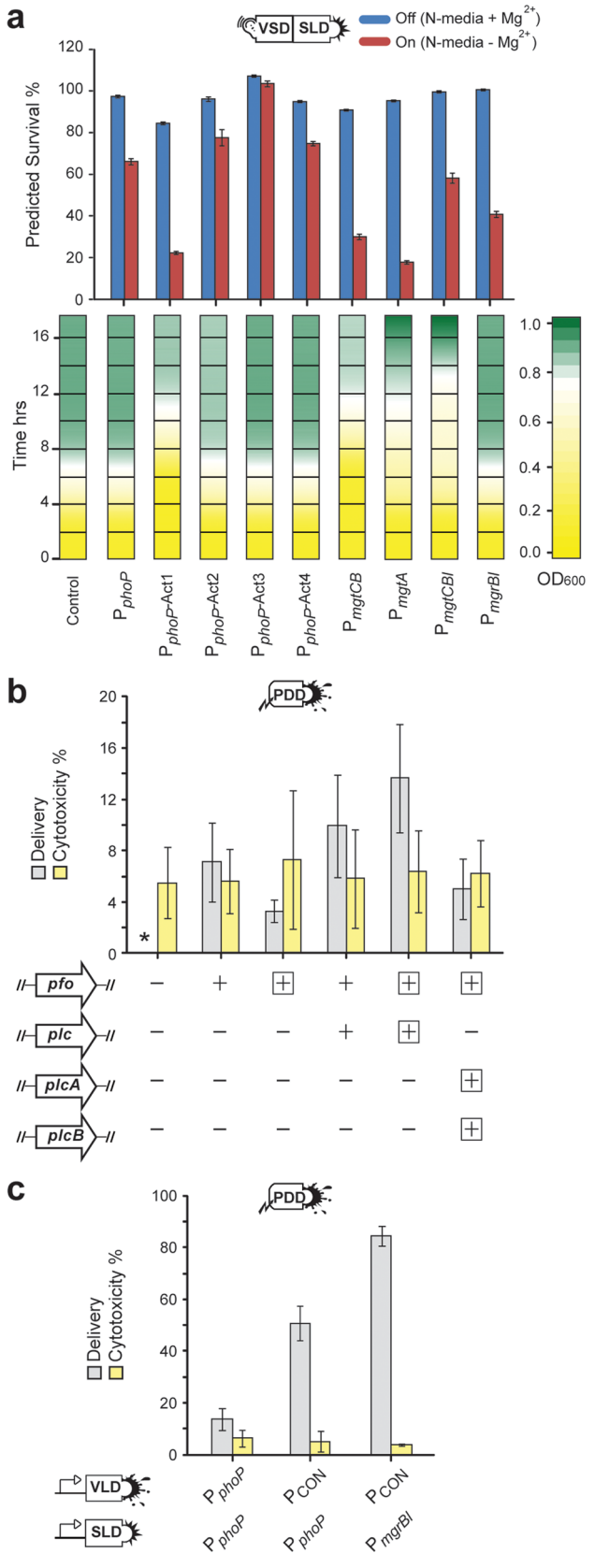

Figure 4. Characterization of the composed devices. (a) The degree of lysis from the VSD and SLD combinations in both the Off and On state were predicted, with error bars calculated from the standard deviation of the relative transcription measurements of the VSD. Growth curves of devices in LB + Mg^{2+} were also measured; the mean of 4 replicates is illustrated. (b) Fluorescent protein payloads were

dx.doi.org/10.1021/sb300107h | ACS Synth. Biol. 2013, 2, 418−424

Figure 4. continued

delivered to U373 MG cells *in vivo*, and the efficiency of delivery and cytotoxicity was measured for each VLD variant. (+): device installed. Boxed (+): device with degradation tag installed. (−): device not installed. Error bars indicate the standard deviation of 3 biological replicates. (c) Payload delivery was evaluated using different promoters to drive the VLD and SLD. Error bars indicate the standard deviation of 3 biological replicates.

low basal self-lysis activity. Unexpectedly, the device combinations using P_{mgtA} and P_{mgtCBI} grew slowly and eventually exceeded the cell density of a device-free control. Because this behavior was inconsistent with the behavior of other devices, we did not consider them for further integration and testing. We selected P_{mgrBI} to evaluate in the complete system because of its stability and high predicted activity. Consistent with this prediction, replacement of the P_{phoP} VSD module with the P_{mgrBI} VSD module improved payload delivery efficiency to over 80% (Figure 4c). In addition to laying the groundwork for development of a tumor-killing therapeutic, this high level of macromolecular delivery opens the doors for other therapeutic applications, such as modification of the host genome.

The basic premise of modular design is that low-level devices can be built, tested, and then later merged into larger systems. If this holds for cellular systems, then it should be possible to independently construct genetic devices and then combine them for higher-order behavior in the cell. The design, fabrication, and testing of each low-level device was readily achieved by drawing on existing information about biological components. Although integrating low-level devices together revealed some unanticipated behaviors, these behaviors were readily addressed by simple design modifications, resulting in a functional system. We expect that such contextual effects are generally finite, traceable to specific mechanisms and, ultimately, addressable by good design. For example, exploration of a genetic circuit employing T7 polymerase to generate a positive feedback loop revealed that a quantifiable interaction with the host generated bistability, despite the lack of a cooperative interaction.[35] Even absent specific mechanistic explanations of host-system interactions, empirical observations about the relationship between gene expression and cellular growth can guide system manipulation.[36] Taken together, these observations suggest that modular design is a viable strategy for the design of genetic systems.

Further, we were able to predict an improved system composition based on measurements of the underlying modules and subsystems. Although quantification of module behavior was only employed here for optimization, we expect that improvements in our ability to measure and quantify cellular processes will enable *in silico* specification of effective systems based on single-module measurements. Such a simplification of the design process should lead to a corresponding increase in the complexity of engineered genetic systems.

METHODS

Plasmids and Strains. The genetic constructs used in this study are diagramed in Figure 1b and were constructed using BglBrick standard assembly,[37] a variation on BioBrick standard assembly using the *Bgl*II and *Bam*HI restriction enzymes. To facilitate part assembly, methylating strains of *E. coli* were employed.[38] All experiments were performed with *E. coli* strains MG1655, MC1061, and derivatives thereof (Supplementary Table 4). Sequences of DNAs used to fabricate composite devices are available in the MIT Registry of Standard Biological Parts (http://partsregistry.org). The complete composition of devices is available in Supplementary Table 2.

Growth Medium and Condition. *E. coli* were grown in Luria Broth (LB) medium for routine molecular biology protocols. Cultures for assay experiments were grown in LB, LB supplemented with 30 mM $MgSO_4$ (LB + Mg^{2+}), N-minimal medium[39] supplemented with 0.1% casamino acids, 38 mM glycerol (N-medium), and 30 mM or 0 mM $MgSO_4$ (N-medium ± Mg^{2+}), or Terrific Broth (TB) supplemented with 30 mM of $MgSO_4$ (TB + Mg^{2+}). Cultures were incubated at 37 °C with 700 rpm shaking in a Multitron Standard orbital plate shaker (Infors-HT, Bottmingen, Switzerland).

Relative Transcription Determination. Relative transcription was determined essentially as described previously,[40] except that cells were assayed under specific, nonlogarithmic growth conditions. Briefly, samples of stationary phase bacteria grown in LB + Mg^{2+} bearing a plasmid with either a constitutive standard reference promoter (P_{REF}) or a test promoter (P_{TEST}) driving expression of green fluorescent protein were subcultured 1:100 into fresh LB + Mg^{2+} and grown until reaching an OD_{600} of 0.5. They were subsequently washed twice with N-medium ± Mg^{2+} and resuspended in the same medium. They were then incubated at 37 °C for 6.5 h, and the OD_{600} (OD) and fluorescence intensity (F; excitation 501 nm, emission 511 nm) measured with a fluorescent plate reader. Relative transcription was then calculated as $\{F(P_{TEST})/OD(P_{TEST})\}/\{F(P_{REF})/OD(P_{REF})\}$.

Assay for Self-Lysis Activity. *E. coli* bearing an arabinose-inducible promoter (P_{BAD}) driven SLD were grown to stationary phase in LB + Mg^{2+}. They were then diluted 1:100 into fresh LB + Mg^{2+} medium and grown to an OD_{600} of 0.5. Bacteria were collected by centrifugation, washed twice with N-medium ± Mg^{2+} and resuspended to an OD_{600} of 0.5 in N-medium ± Mg^{2+} containing 0−1.33 mM arabinose. They were incubated at 37 °C for 6.5 h, and the OD_{600} was measured with a plate reader. Percent survival was calculated as sample OD_{600} divided by control OD_{600} (*E. coli* without SLD), and arabinose concentration was mapped to relative transcription (see Supporting Information).

Growth Curve Determination. *E. coli* bearing VSDs driving a SLD or a plasmid-less control were grown to stationary phase in LB + Mg^{2+}. These were subcultured 1:100 into fresh LB + Mg^{2+}, and a 200 μL aliquot was transferred to a Corning flat-bottom 96-well microplate. The plate was incubated at 37 °C, and the OD_{600} was measured every 5 min.

Microscopy of Devices. A monolayer of HeLa or U373 MG cells was prepared 24 h prior to experimentation on an 8-well chambered slide (LabTech) in growth medium (DMEM supplemented with 10% fetal bovine serum (FBS) for HeLa and DMEM supplemented with 1% nonessential amino acids (NEAA), 1 mM sodium pyruvate, and 10% FBS for U373 MG) with penicillin and streptomycin antibiotics. The medium was replaced with fresh medium without antibiotics, and stationary phase bacterial culture (grown in TB + Mg^{2+}) was added to each well. For experiments without a VLD, 1 μL of bacteria and HeLa were used, resulting in an average of 20−80 internalized bacteria per mammalian cell, while for experiments with a VLD, 0.5 μL of bacteria and U373 MG were used, resulting in an average of 1−3 internalized bacteria per mammalian cell. After 80 min of incubation at 37 °C, cells were washed twice into

growth medium with 100 μg/mL gentamicin, and the slides were incubated for a further 3.5 h before examination by microscopy. Images were taken with Zeiss Axiobserver D1 or Zeiss Axiovision Z1 inverted microscope equipped with Hamamatsu 9100-13 EMCCD camera. For complete PDD, the delivery efficiency was quantified as the number cells with a green nucleus divided by the number of cells bearing internalized bacteria and/or a green nucleus. To determine cytotoxicity after the 3.5 h incubation, each well was incubated with PBS containing a final concentration of 4 μM of ethidium homodimer-1 (EthD-1) (Life Technologies) and 2 μM of Hoechst 33342 (VWR) for 10 min at 37 °C. EthD-1 stains the nucleus of membrane permeabilized (dead) cells and Hoechst stains the nucleus of all cells. Cytotoxicity was calculated as the number of EthD-1 stained cells divided by the number of cells bearing internalized bacteria and/or a green nucleus.

Biosafety and Biosecurity Considerations. All experiments followed the guidelines of the Office of Environment, Health, and Safety (EH&S) at UC Berkeley. Since many of the strains used in these studies involved virulence factors from risk group 2 (RG2) organisms, these materials are regarded as RG2, and our work operated under biosafety level 2 protocols. High affinity iron transport mutants (Δ*tonB*) were employed to mitigate any risks to researchers or the environment posed by these organisms. To mitigate potential dual use of these materials, only the RG1 parts are fully described at base-level precision. Full sequences including RG2 components and physical DNAs are available upon request from researchers presenting evidence of institutional approval.

■ ASSOCIATED CONTENT

Supporting Information

Further results and discussion, including supplemental Figures 1, 2, and 3, and a list of parts, plasmids, and strains used for the study. This material is available free of charge via the Internet at http://pubs.acs.org.

■ AUTHOR INFORMATION

Corresponding Author

*E-mail: jcanderson@berkeley.edu.

Author Contributions

J.H.H. designed and performed the experiments, analyzed the data, and wrote the manuscript. J.T.K. analyzed the data and wrote the manuscript. A.P.A. and J.C.A. designed experiments, analyzed the data, and wrote the manuscript.

Notes

The authors declare no competing financial interest.

■ ACKNOWLEDGMENTS

We thank the CNR Biological Imaging Facility (University of California, Berkeley) for assistance in microscopy. We also thank Lon Chubiz for providing a CRIM helper plasmid for integrating DNA into the attP21 site of the *E. coli* genome. This work was supported by the National Science Foundation Synthetic Biology Engineering Research Center (SynBERC). J.T.K. received support from a National Science Foundation Graduate Research Fellowship and a Siebel Scholar award.

■ ABBREVIATIONS

PLD, payload device; ID, invasion device; VSD, vacuole sensing device; SLD, self-lysis device; VLD, vacuole lysis device; DAP, diaminopimelic acid

■ REFERENCES

(1) Khalil, A. S., and Collins, J. J. (2010) Synthetic biology: applications come of age. *Nat. Rev. Genet. 11*, 367−379.

(2) Endy, D. (2005) Foundations for engineering biology. *Nature 438*, 449−453.

(3) Purnick, P. E., and Weiss, R. (2009) The second wave of synthetic biology: from modules to systems. *Nat. Rev. Mol. Cell Biol. 10*, 410−422.

(4) Prather, K. L., and Martin, C. H. (2008) De novo biosynthetic pathways: rational design of microbial chemical factories. *Curr. Opin. Biotechnol. 19*, 468−474.

(5) Tabor, J. J., Salis, H. M., Simpson, Z. B., Chevalier, A. A., Levskaya, A., Marcotte, E. M., Voigt, C. A., and Ellington, A. D. (2009) A synthetic genetic edge detection program. *Cell 137*, 1272−1281.

(6) Wang, B., Kitney, R. I., Joly, N., and Buck, M. (2011) Engineering modular and orthogonal genetic logic gates for robust digital-like synthetic biology. *Nat. Commun. 2*, 508.

(7) Seow, Y., and Wood, M. J. (2009) Biological gene delivery vehicles: beyond viral vectors. *Mol. Ther. 17*, 767−777.

(8) Courvalin, P., Goussard, S., and Grillot-Courvalin, C. (1995) Gene transfer from bacteria to mammalian cells. *C. R. Acad. Sci., Ser. III 318*, 1207−1212.

(9) Larsen, M. D., Griesenbach, U., Goussard, S., Gruenert, D. C., Geddes, D. M., Scheule, R. K., Cheng, S. H., Courvalin, P., Grillot-Courvalin, C., and Alton, E. W. (2008) Bactofection of lung epithelial cells in vitro and in vivo using a genetically modified Escherichia coli. *Gene Ther. 15*, 434−442.

(10) Forbes, N. S. (2010) Engineering the perfect (bacterial) cancer therapy. *Nat. Rev. Cancer 10*, 785−794.

(11) van Pijkeren, J. P., Morrissey, D., Monk, I. R., Cronin, M., Rajendran, S., O'Sullivan, G. C., Gahan, C. G., and Tangney, M. (2010) A novel Listeria monocytogenes-based DNA delivery system for cancer gene therapy. *Hum. Gene Ther. 21*, 405−416.

(12) Yazawa, K., Fujimori, M., Nakamura, T., Sasaki, T., Amano, J., Kano, Y., and Taniguchi, S. (2001) Bifidobacterium longum as a delivery system for gene therapy of chemically induced rat mammary tumors. *Breast Cancer Res. Treat. 66*, 165−170.

(13) Sizemore, D. R., Branstrom, A. A., and Sadoff, J. C. (1995) Attenuated Shigella as a DNA delivery vehicle for DNA-mediated immunization. *Science 270*, 299−302.

(14) Zhu, X., Cai, J., Huang, J., Jiang, X., and Ren, D. (2010) The treatment and prevention of mouse melanoma with an oral DNA vaccine carried by attenuated Salmonella typhimurium. *J. Immunother. 33*, 453−460.

(15) Grillot-Courvalin, C., Goussard, S., Huetz, F., Ojcius, D. M., and Courvalin, P. (1998) Functional gene transfer from intracellular bacteria to mammalian cells. *Nat. Biotechnol. 16*, 862−866.

(16) Baban, C. K., Cronin, M., O'Hanlon, D., O'Sullivan, G. C., and Tangney, M. (2011) Bacteria as vectors for gene therapy of cancer. *Bioeng. Bugs 1*, 385−394.

(17) Fajac, I., Grosse, S., Collombet, J. M., Thevenot, G., Goussard, S., Danel, C., and Grillot-Courvalin, C. (2004) Recombinant Escherichia coli as a gene delivery vector into airway epithelial cells. *J. Controlled Release 97*, 371−381.

(18) Castagliuolo, I., Beggiao, E., Brun, P., Barzon, L., Goussard, S., Manganelli, R., Grillot-Courvalin, C., and Palu, G. (2005) Engineered E. coli delivers therapeutic genes to the colonic mucosa. *Gene Ther. 12*, 1070−1078.

(19) Kalderon, D., Roberts, B. L., Richardson, W. D., and Smith, A. E. (1984) A short amino acid sequence able to specify nuclear location. *Cell 39*, 499−509.

(20) Anderson, J. C., Clarke, E. J., Arkin, A. P., and Voigt, C. A. (2006) Environmentally controlled invasion of cancer cells by engineered bacteria. *J. Mol. Biol. 355*, 619−627.

(21) Isberg, R. R., and Van Nhieu, G. T. (1995) The mechanism of phagocytic uptake promoted by invasin-integrin interaction. *Trends Cell Biol. 5*, 120−124.

(22) Young, V. B., Falkow, S., and Schoolnik, G. K. (1992) The invasin protein of Yersinia enterocolitica: internalization of invasin-

bearing bacteria by eukaryotic cells is associated with reorganization of the cytoskeleton. *J. Cell Biol. 116*, 197−207.
(23) Ernst, R. K., Guina, T., and Miller, S. I. (1999) How intracellular bacteria survive: surface modifications that promote resistance to host innate immune responses. *J. Infect. Dis. 179* (Suppl 2), S326−330.
(24) Garcia Vescovi, E., Soncini, F. C., and Groisman, E. A. (1996) Mg2+ as an extracellular signal: environmental regulation of Salmonella virulence. *Cell 84*, 165−174.
(25) White, R., Chiba, S., Pang, T., Dewey, J. S., Savva, C. G., Holzenburg, A., Pogliano, K., and Young, R. (2011) Holin triggering in real time. *Proc. Natl. Acad. Sci. U.S.A. 108*, 798−803.
(26) Tran, T. A., Struck, D. K., and Young, R. (2005) Periplasmic domains define holin-antiholin interactions in t4 lysis inhibition. *J. Bacteriol. 187*, 6631−6640.
(27) Buchler, N. E., and Cross, F. R. (2009) Protein sequestration generates a flexible ultrasensitive response in a genetic network. *Mol. Syst. Biol. 5*, 272.
(28) Zhang, N., and Young, R. (1999) Complementation and characterization of the nested Rz and Rz1 reading frames in the genome of bacteriophage lambda. *Mol. Gen. Genet. 262*, 659−667.
(29) O'Brien, D. K., and Melville, S. B. (2004) Effects of Clostridium perfringens alpha-toxin (PLC) and perfringolysin O (PFO) on cytotoxicity to macrophages, on escape from the phagosomes of macrophages, and on persistence of C. perfringens in host tissues. *Infect. Immun. 72*, 5204−5215.
(30) Smith, G. A., Marquis, H., Jones, S., Johnston, N. C., Portnoy, D. A., and Goldfine, H. (1995) The two distinct phospholipases C of Listeria monocytogenes have overlapping roles in escape from a vacuole and cell-to-cell spread. *Infect. Immun. 63*, 4231−4237.
(31) Decatur, A. L., and Portnoy, D. A. (2000) A PEST-like sequence in listeriolysin O essential for Listeria monocytogenes pathogenicity. *Science 290*, 992−995.
(32) Mogk, A., Schmidt, R., and Bukau, B. (2007) The N-end rule pathway for regulated proteolysis: prokaryotic and eukaryotic strategies. *Trends Cell Biol. 17*, 165−172.
(33) Luzio, J. P., Bright, N. A., and Pryor, P. R. (2007) The role of calcium and other ions in sorting and delivery in the late endocytic pathway. *Biochem. Soc. Trans. 35*, 1088−1091.
(34) Luirink, J., van der Sande, C., Tommassen, J., Veltkamp, E., De Graaf, F. K., and Oudega, B. (1986) Effects of divalent cations and of phospholipase A activity on excretion of cloacin DF13 and lysis of host cells. *J. Gen. Microbiol. 132*, 825−834.
(35) Tan, C., Marguet, P., and You, L. (2009) Emergent bistability by a growth-modulating positive feedback circuit. *Nat. Chem. Biol. 5*, 842−848.
(36) Scott, M., Gunderson, C. W., Mateescu, E. M., Zhang, Z., and Hwa, T. (2010) Interdependence of cell growth and gene expression: origins and consequences. *Science 330*, 1099−1102.
(37) Anderson, J. C., Dueber, J. E., Leguia, M., Wu, G. C., Goler, J. A., Arkin, A. P., and Keasling, J. D. (2010) BglBricks: A flexible standard for biological part assembly. *J. Biol. Eng. 4*, 1.
(38) Leguia, M., Brophy, J., Densmore, D., and Anderson, J. C. (2011) Automated assembly of standard biological parts. *Methods Enzymol. 498*, 363−397.
(39) Kato, A., and Groisman, E. A. (2004) Connecting two-component regulatory systems by a protein that protects a response regulator from dephosphorylation by its cognate sensor. *Genes Dev. 18*, 2302−2313.
(40) Kelly, J. R., Rubin, A. J., Davis, J. H., Ajo-Franklin, C. M., Cumbers, J., Czar, M. J., de Mora, K., Glieberman, A. L., Monie, D. D., and Endy, D. (2009) Measuring the activity of BioBrick promoters using an in vivo reference standard. *J. Biol. Eng. 3*, 4.